Surface and Interface Characterization of Untreated and SMA Imide-Treated Hemp Fiber/Acrylic Composites

Tayebeh Behzad,[1] **Mohini Sain**[2]
[1]*Department of Chemical Engineering and Applied Chemistry, University of Toronto, Toronto, Canada*

[2]*Department of Chemical Engineering and Applied Chemistry/Forestry, University of Toronto, Toronto, Canada*

The hydrophilic nature of natural fibers adversely affects adhesion to a hydrophobic matrix, and consequently it may unfavorably influence the strength of the composite. Therefore, modifying the fiber or the matrix is essential to obtain optimum composite properties. In this work, hemp fibers were modified applying a paper sizing technique using SMA Imide resin (copolymer of styrene and dimethylaminopropylamine maleimide) as a surface modifying agent. The performance of the hemp/acrylic composite was improved significantly using the treated fibers. Inverse gas chromatography (IGC) and pull-out test were employed to study the hemp fiber/matrix interface and the surface characteristics of untreated and treated hemp fibers. The IGC results demonstrated that treated fibers had slightly higher dispersive force compared with untreated fibers. Moreover, modification of fibers with SMA Imide resin slightly decreased the basic character and significantly increased the acid character of hemp fibers. From the pull-out test, the average stress to pull the SMA-treated fibers out was 71% higher than that calculated for untreated fibers. The higher interfacial strength for the treated fibers shows that the SMA treatment had a beneficial influence on the adhesion of the acrylic resin to the hemp fibers. POLYM. COMPOS., 30:681–690, 2009. © 2009 Society of Plastics Engineers

INTRODUCTION

Over the past few years, development of natural fiber composites has been an interesting subject for scientists and industries. These materials were made through the combination of natural fibers with different plastics. These composite materials now dominate the furniture, housing, construction, transportation, and sporting industries [1–3]. The physical and mechanical properties of fiber composites mainly depend on the fiber loading, the individual properties of the fiber and matrix, and the fiber/matrix adhesion. Concerning the interfacial interaction, the hydrophilic nature of natural fibers adversely affects adhesion to a polymer matrix, and consequently it may unfavorably influence the strength of the composite. Therefore, modifying the fiber or the matrix, or both, is essential to obtain optimum composite properties.

Chemical methods have been widely used to modify the surface properties of natural fibers. Chemical modifications improve the fiber compatibility with, and dispersion into, the matrix, which improves the stress transfer at the fiber/matrix interface. There are different chemical techniques developed, such as silane treatment, alkalization, isocyanate treatment, and graft copolymerization [4–7].

There are several methods to characterize the fiber surface and fiber/matrix interface properties, but two are of particular interest here. The first method is inverse gas chromatography (IGC), which is convenient for evaluating surface characteristics of polymers and reinforcing fibers. IGC is used to determine the dispersive component of the surface energy and acid–base characteristics of the materials [8, 9]. Kamdem [10] applied IGC to characterize the surface of brich wood meal by estimating the dispersive force and the acid/base characters of wood. The results proved the presence of both acidic and basic sites on the wood surface; however, the acidic character was more predominant. Tshablala [11] studied the surface acid–base characteristics of cellulose, pine wood, and kenaf powder using IGC. The results indicated that the surface of washed pine wood and kenaf articles had amphoteric behavior with more acidic capacity. On the contrary, the nonwashed wood had a neutral surface, and nonwashed kenaf appeared to be basic because of the presence of triglycerides on the surface. The cellulose powder presented a predominantly acidic character. Moreover, the removal of extractives by treatment increased the dispersive component of the surface energy of the pine wood and kenaf particles. In another work, the acid–base characteristics

Correspondence to: Mohini Sain; e-mail: m.sain@utoronto.ca
Contract grant sponsor: Network of Center of Excellence-Auto 21, Canada.
DOI 10.1002/pc.20418
Published online in Wiley InterScience (www.interscience.wiley.com).

and dispersion component of surface energy of untreated and modified hemp fibers were determined by Gulati [12]. Alkalization and acetylation increased the dispersive component of hemp fiber because of dissolution of impurities and exposure of relatively higher energy cellulose. Alkalization increased the acidic character and reduced the basic character of the surface due to the exposure of cellulose. On the other hand, acetylation was found to decrease the basic character of hemp fibers because of dissolution of extractives. Mechanical performance of the hemp fiber/unsaturated polyester composite showed the highest improvement for alkali-treated fibers due to high acid–base interactions.

The second, pull-out testing, is a method to measure the shear strength of the fiber/matrix interface. A single fiber is embedded in a matrix block, and an increasing force is applied to the free end of the fiber to pull it out of the matrix. The shear strength at the interface can be calculated using the tensile strength, the embedded length, and the diameter of the fiber. For instance, the improvement of the adhesion of polyethylene terephthalate fibers to polyhydroxyethyl methacrylate hydrogels by ozone treatment was studied by Ferreira et al. [13] using pull-out test. The interfacial shear strength on hydrogels was 65% higher for ozonated treated fibers than untreated fibers because of the presence of different functionalities such as carboxylic, anhydride, and hydroxyl groups. Wood veneer pull-out test was performed to evaluate the interfacial adhesion of both untreated and treated wood veneer bonded with polypropylene by Kazayawoko et al. [14]. The interfacial shear strength was higher for combed wood veneer, which has a rough surface compared with the untreated wood veneer. The roughening of the wood veneer surface exposes more surface area, which increases interfacial mechanical interlocking as well. Chand and Rohatgi [15] studied the effect of alkali treatment on the surface adhesion of sisal fibers to polyester resin using pull-out test. The results showed that as the soaking time was increased from 0 to 90 h, the pull-out loads increased from 10 to 15.5 N and hence the adhesion increased. Further increasing in the soaking time above 96 h resulted in a gradual decrease in the pull-out load. In another work, the effect of sodium hydroxide and *N*-isopropyl-acrylamide solution on the interfacial adhesion of sisal/polyester was studied by Sydenstricker and Mochnaz [16]. All treatments improved the interfacial adhesion between sisal and polyester; however, 2% NaOH and 2% acrylamide treatments demonstrated the best choice.

In this work, the hemp fiber surface was treated employing a paper sizing technique using SMA Imide resin as a surface modifying agent. The hemp fiber/acrylic composites were manufactured using untreated and treated hemp fibers, and their performances were evaluated. The effect of treatment on surface characteristics of hemp fiber was studied using IGC. Additionally, the untreated and treated fiber/matrix interface was studied using a pull-out test.

EXPERIMENTAL PROCEDURES

Materials

An environmental friendly thermoset water-based acrylic polymer was obtained from BASF Canada (Ontario). The polymer is an aqueous solution of a polycarboxylic acid and a polyhydric alcohol as a crosslinking agent in water (52% water). Hemp in the form of randomly oriented loose fibers was supplied by Hempline Canada (Ontario). The average fiber length was 9 cm and the diameter of the fiber was in the range of 10–300 μm. For the chemical treatment of fibers, the SMA Imide resin 3000I (copolymer of styrene and dimethylaminopropylamine maleimide) was obtained from ATOFINA Canada (Ontario). The IGC probes used in this study were *n*-hexane (99%), *n*-heptane (99%), *n*-octane (97%), *n*-nonane (99%), chloroform (99.8%), ethylether (99.5%), ethylacetate (99.5%), and acetone (99.5%). All of these probes were obtained from Caledon Laboratories, Canada (Ontario).

Fiber Treatment

A solution of SMA Imide resin 3000I was prepared by dissolving the powder in water at 60°C until it completely dissolved. For preparation of the sizing system, some acetic acid was added to the hot solution. A concentration of 1.5 wt% of SMA was prepared and the fibers were soaked overnight. The fibers were dried at 60°C for 24 h.

Fiber Diameter and Strength Measurements

The diameters of both untreated and treated fibers prepared by the procedure were measured using the following procedure. First, thin hemp fibers with sufficient length were selected from the fiber bunch. A small window with the dimension of 1×1 cm^2 was cut in the middle of a piece of paper. The hemp fiber was pulled across the window and fixed to the paper by an adhesive tape. The diameters of the fibers were measured at three points inside the window using a reflectance light microscope to calculate the average value.

Strength of the untreated and treated fibers was measured using Sintech 1 tensile machine with a 22.7 kg load cell with a head speed of 5 mm $\cdot$ min^{-1}. The distance between the upper and lower grips was fixed to 1 cm. The paper with fiber was gripped to the machine. The middle part of the paper was cut carefully before testing.

Composite Preparation

Nonwoven loose hemp fibers were randomly oriented in a Buchner funnel manually. The funnel was connected to a vacuum system. A diluted resin solution with 10 wt% resin content was prepared by adding the solvent to

 DOI 10.1002/pc

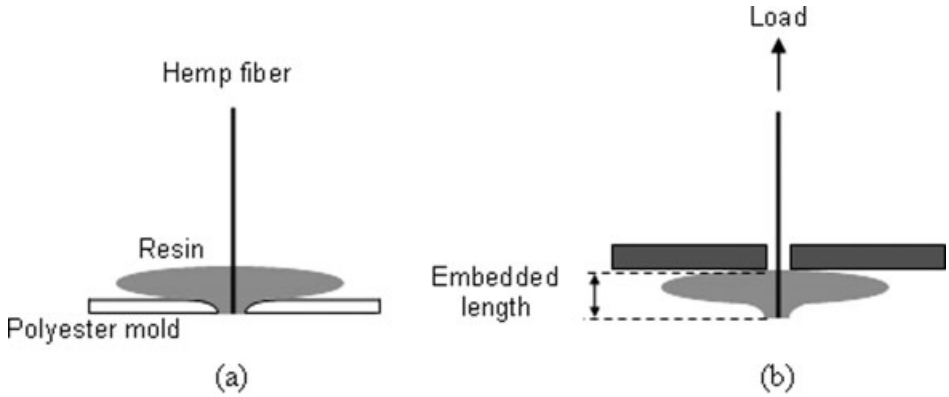

FIG. 1. (a) Single fiber pull-out test specimen, (b) experimental arrangement for pull-out test.

the resin to circulate through the fibers. The outlet of funnel was blocked, and the resin solution was spread all over the fibers. To ensure a complete impregnation of the solution through the fibers, the solution was circulated a few times. In the last stage, a vacuum pressure was applied to drain the excess solution. After the circulation of the resin solution, the wet mat was removed from the funnel and placed on a nonstick polyester sheet and then kept in an oven at 55°C for 48 h to remove all the moisture content. The mat would be ready for the compression molding process at optimum cure conditions after the drying cycle [17].

Mechanical Test

Composite panels were cut into sections allowing for at least three tensile and flexural test specimens in each case. The tensile properties of the composites were measured following the ASTM standard method (D-638) [18]. The flexural properties were obtained according to the ASTM standard method (D-790) [19].

Scanning Electron Microscope

The scanning electron microscope (SEM) Hitachi S-570 was employed to take SEM micrographs to analyze the treated and untreated hemp fibers and the fracture surface of the treated and untreated composites.

Column Preparation and IGC Procedure

The hemp fibers were prepared by grinding in a wiley mill to a 60-mesh size. A cupper column 33 cm long with 4 mm internal diameter was cut and washed with methanol and methylene chloride to remove any grease inside the column. The column was connected to an air supply to vaporize any solvents and then placed in an oven at 100°C for 1 h. Once the column was dry, it was packed with almost 2 g of hemp fibers by blocking one end of the column with glass wool and applying suction to fill the column.

IGC measurements were carried out using a Perkin-Elmer gas chromatograph equipped with a thermal conductivity detector. The hemp-filled column was carefully bent and hooked to the machine. Helium was used as a carrier gas at the flow rate of 10 $ml \cdot min^{-1}$ and was corrected for pressure drop along the column. The exact flow rate was calculated for each measurement by a digital flow meter. The temperature of the inlet port was set at 200°C to ensure flash vaporization of the liquid probes. The column outlet was at atmospheric pressure, which was obtained from a digital barometer. The column was conditioned overnight with helium flowing through it. Individual samples of chemical probes (0.05 μl) were injected directly into the carrier gas stream. Methane was selected to measure the dead volume of the column. Measurements were performed in temperatures between 40 and 100°C in 20°C increments. The chromatographic peaks were generally symmetrical.

Pull-Out Test

The number of test specimens was 100 for treated, as well as for the untreated fibers. The diameter of fibers was measured as discussed in the previous section (Fiber Diameter and Strength Measurements). Single fiber pull-out specimens were prepared as shown in Fig. 1a. A single fiber was partially embedded in the resin. To prevent fiber breakage during the pulling, the embedded length of the fiber in the matrix should be very small [20]. To properly embed the fiber, a mold of polyester sheet was made with a thickness and diameter of 100 μm and 1 mm, respectively.

A single drop of the resin was placed on the mold with a final thickness of less than 600 μm, as illustrated in Fig. 1a. A single fiber was then inserted in the mold. The pull-out specimens were cured after the drying cycle. The total embedded length was kept between 150 and 700 μm. The cured samples were removed from the polyester mold and uniaxially loaded in tension until pull-out occurs, as shown in Fig. 1b. The fiber-free length between the matrix and the grip was $\sim$5 mm. Fiber pull-out tests

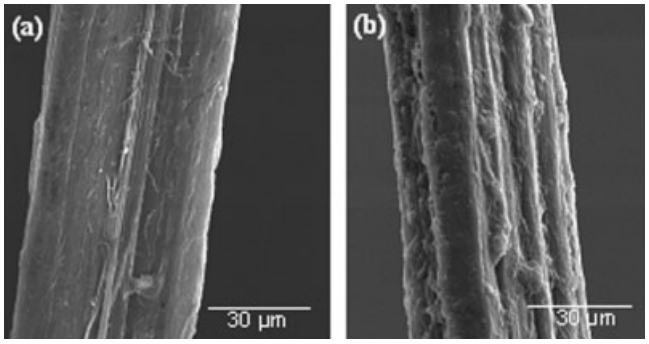

FIG. 2. SEM micrographs of hemp fiber: (a) untreated, (b) SMA Imide treated.

were carried out at a cross-head speed of 1 $mm \cdot min^{-1}$ and a load cell of 2.2 kg.

RESULTS AND DISCUSSION

Scanning Electron Microscope

Hemp-bundle fibers consist of single fibers adhered together by lignin. In an effort to improve the interfacial adhesion in acrylic composites, hemp fibers were submitted to a surface treatment using SMA Imide resin as a surface modifier. The micrographs of untreated and treated hemp-fiber surfaces are shown in Fig. 2. The untreated hemp fibers consist of bundles of individual cells that are bounded together by lignin (Fig. 2a). In general, the treated surfaces look different from that of the untreated hemp fibers. The SMA treatment shows some disaggregation of fiber bundles and some roughness on the surfaces, which can be due to the deposition of SMA on the surface of hemp fibers.

Strength of Untreated and SMA-Treated Fibers

To study the effect of SMA Imide treatment on the performance of the fiber, the tensile properties of the untreated and SMA Imide-treated fibers were measured. Figures 3 and 4 show the tensile strength and modulus of the untreated and treated fibers. The student's *t*-test showed that at a 95% confidence level, there is no statistically significant difference between tensile properties of the untreated and treated fibers. This means that the SMA Imide treatment does not change the performance of the fibers.

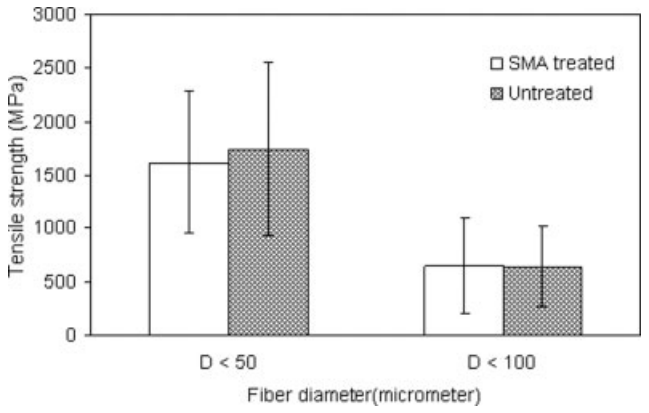

FIG. 3. Tensile strength of untreated and SMA Imide treated fibers.

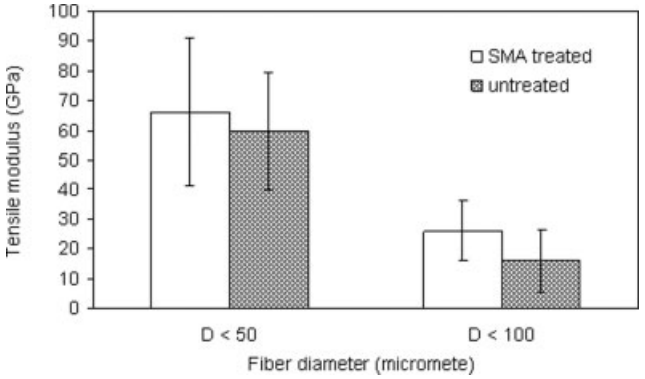

FIG. 4. Tensile modulus of untreated and SMA Imide treated fibers.

Mechanical Properties

Figures 5 and 6 present the strength and modulus of the treated and untreated samples. It is clear that the treated fibers led to almost a 26% increase in both the average tensile and flexural strength and a 34 and 10% increase in the average value of tensile and flexural modulus of the composite, respectively. The ANOVA statistical analysis was performed at 95% confidence level and it was found that the strength and tensile modulus of the SMA treated composite are significantly higher than the untreated composite ($P < 0.02$). SMA Imide resins contain a high level of functionality (Fig. 7), which can instigate a chemical interaction between the fiber and matrix, resulting in a good interaction between the hydrophilic fiber and matrix.

Fracture Surface

Evidence of improved interfacial adhesion reflected by the tensile fracture surface of the treated fiber and matrix is shown by SEM micrographs (Fig. 8). For the untreated

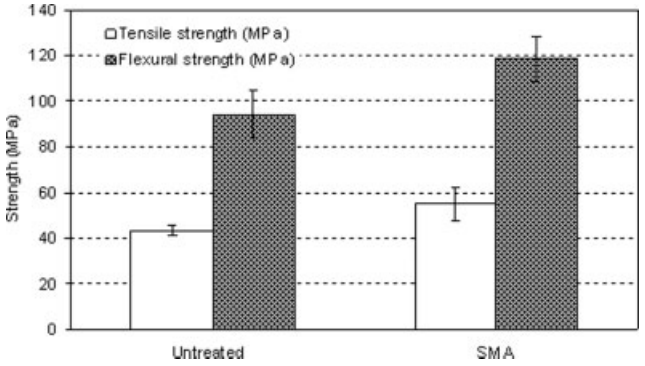

FIG. 5. Strength of untreated and treated composite.

DOI 10.1002/pc

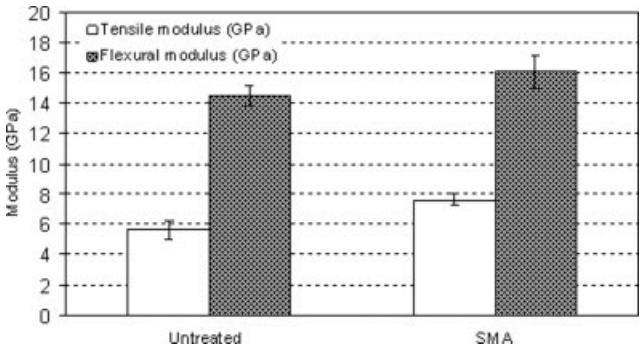

FIG. 6. Modulus of untreated and treated composite.

hemp fibers, the fracture surfaces of the composites were very fibrous in appearance with high numbers of fiber pull-outs (Fig. 8a). In contrast, a fairly smooth surface was observed for SMA-treated fibers with less debonding (Fig. 8b).

IGC and Thermodynamic Data

Dispersions and acid–base characteristics of solid surfaces play an important role in the interaction of solids with liquids and, in fact, are the primary forces responsible for adhesion. According to Fowkes, the total work of adhesion is obtained as follows [21]:

$$W_a = W_a^d + W_a^{AB} \tag{1}$$

where W_a, W_a^d, and W_a^{AB} are the total work of adhesion, work of adhesion due to the dispersion force, and work of adhesion due to the acid–base interaction, respectively. From a thermodynamic point of view, the adhesion strength between the matrix and fiber is enhanced considerably by increasing the thermodynamic work of adhesion, which is affected mainly by dispersive (nonpolar) and acid–base (polar) interactions.

IGC has been widely used to study the thermodynamics of adsorption and the surface properties of materials [22, 23]. In this technique, the surface of the solid is characterized by injection of probes of known properties into the column containing the solid. To determine the interactions between the probes and the solid, the retention times

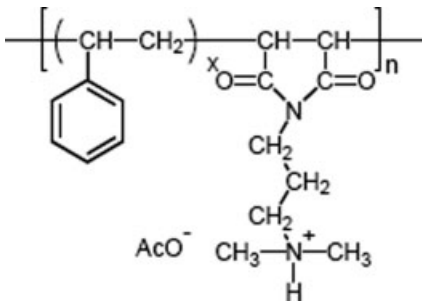

FIG. 7. SMA Imide cationic salt structure.

of the probes at infinite dilution is measured. The net retention volume, V_n, is calculated as follows [24]:

$$V_n = jF(t_n - t_r) \tag{2}$$

where F is the carrier gas flow rate, t_n is the retention time of the given probe, t_r is the retention time of the noninteracting probes such as methane or air, and j is a correcting factor to consider the gas compressibility factor and is given by:

$$j = \frac{3}{2}\frac{\left(\frac{P_{in}}{P_{out}}\right)^2 - 1}{\left(\frac{P_{in}}{P_{out}}\right)^3 - 1} \tag{3}$$

where P_{in} and P_{out} are the pressure at the inlet and outlet of the column in mmHg [25].

The free energy adsorption per mole of solute, ΔG, is given by [24]:

$$\Delta G = RT \ln V_n + C \tag{4}$$

where R is the gas constant, T is the column temperature, and C is a constant depending on the chosen reference state. According to Schultz et al. [24] ΔG is related to the energy of adhesion, W_a, between the probe and the solid as follows:

$$\Delta G = NaW_a \tag{5}$$

where N is the Avogadro's number and a is the surface area of the probe molecule.

Dispersive and Acid–Base Interactions. Dispersion and acid–base interactions are thought to be independently involved in the adsorption of the probe molecules at the adsorbent surface. According to Fowkes [26], the work of adhesion between solid and liquid, W_a^d, due to the dispersion interaction is given by:

$$W_a^d = 2(\gamma_s^d \gamma_l^d)^{1/2} \tag{6}$$

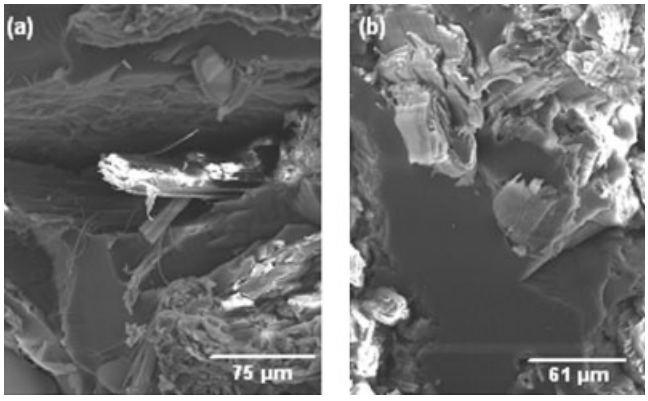

FIG. 8. SEM pictures of tensile fracture surface of the treated hemp fiber/acrylic composites: (a) nontreated, (b) SMA.

TABLE 1. Physicochemical properties of the IGC probes used in this study.

Probe	Area (Å^2)	γ_l^d (mJ/m^2)	DN	AN	Character
Hexane	51.5	18.4	–	–	Neutral
Heptane	57	20.3	–	–	Neutral
Octane	62.8	21.3	–	–	Neutral
Nonane	68.9	22.7	–	–	Neutral
Chloroform	44	25.9	0	23.1	Acidic
Ethyl acetate	48	19.6	17.1	9.3	Amphoteric
Ethyl ether	47	15	19.2	3.9	Basic
Tetrahydrofuran	45	22.5	20	8	Basic
Acetone	42.5	16.5	17	12.5	Amphoteric

where γ_s^d and γ_l^d are the dispersive components of the surface free energies for solid and liquid, respectively. Combining the *Eqs*. 4–6 results to:

$$RT\ \ln(V_n) = 2Na(\gamma_s^d \gamma_l^d)^{1/2} + C \quad (7)$$

This procedure is based on the determination of a linear relationship $RT\ \ln(V_n)$ versus $a\left(\gamma_l^d\right)^{1/2}$ for the series of *n*-alkanes and calculation of γ_s^d from the slope value.

The interaction of polar probes with the surface involves both dispersive and acid–base interactions. To determine the contribution of the acid–base interaction to the total, the contribution of the dispersion interaction can be separated by subtracting the dispersive free energy of adsorption from the alkane line from the global free energy of adsorption. The free energy of adsorption, ΔG^{AB}, corresponding to the specific acid–base interactions, is related to the enthalpy of adsorption, ΔH^{AB}, by the following equation:

$$\Delta G^{AB} = \Delta H^{AB} - T\Delta S^{AB} \quad (8)$$

where ΔS^{AB} is the entropy of adsorption corresponding to the acid–base interaction. A plot of ΔG^{AB} versus T yields a straight line with intercept equal to ΔH^{AB}. The enthalpy

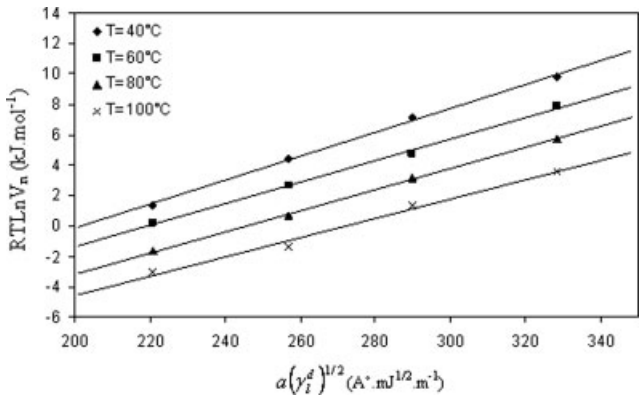

FIG. 9. $RT\ \ln(V_n)$ versus $a\left(\gamma_l^d\right)^{1/2}$ plot for the adsorption of *n*-alkanes on untreated hemp fiber.

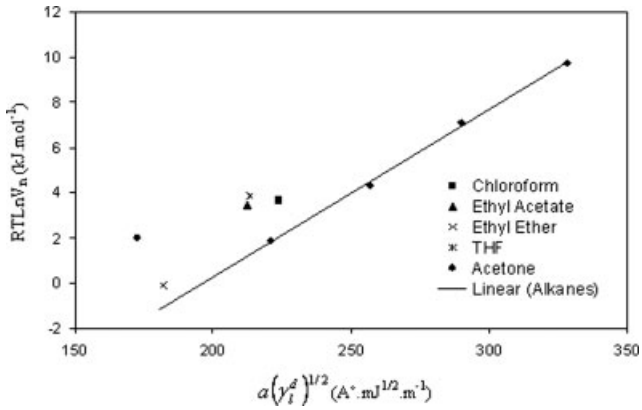

FIG. 10. $RT\ \ln(V_n)$ versus $a\left(\gamma_l^d\right)^{1/2}$ plot for on untreated hemp fiber at 40°C.

of adsorption corresponding to the acid–base interaction is related to the acid and basic parameters, K_A and K_B, of the substrates by the following expression:

$$\Delta H^{AB} = K_A DN + K_B AN \quad (9)$$

where DN and AN are the donor and acceptor numbers, respectively, of the acid–base probe, as defined by Gutmann. A plot of ΔH^{AB}/AN versus DN/AN should result in a straight line with slope K_A and intercept K_B.

Dispersive Component of Untreated and SMA Imide-treated Hemp Fiber. A series of nonpolar *n*-alkanes was used to determine the fiber dispersive surface at different column temperatures. Their physicochemical properties are listed in Table 1.

Plotting of $RT\ \ln V_n$ versus $a\left(\gamma_l^d\right)^{1/2}$, the dispersive component of surface energy for untreated and SMA Imide-treated hemp fibers is calculated from the slope. Figure 9 shows the results for untreated hemp fiber at different temperatures. The excellent linearity of each temperature confirms the validity of *Eq*. 7 for fibers.

All of the polar probes fall off the reference line, indicating that hemp fiber is a solid able to interact with these vapors through non-dispersion forces. Figure 10 shows a plot for the untreated fibers at 40°C. The values for the dispersive component of the surface energy are summarized in Table 2. A decrease of dispersive component at higher temperatures was observed, and the values are sim-

TABLE 2. The dispersive component of surface free energy at different temperatures.

	Dispersive component (mJ/m^2)			
Type of fiber	40°C	60°C	80°C	100°C
Untreated hemp	37 ± 2.5	34 ± 1.8	33 ± 0.4	28 ± 1.6
SMA imide-treated hemp	40 ± 1.15	37 ± 0.65	34 ± 3	33 ± 4

DOI 10.1002/pc

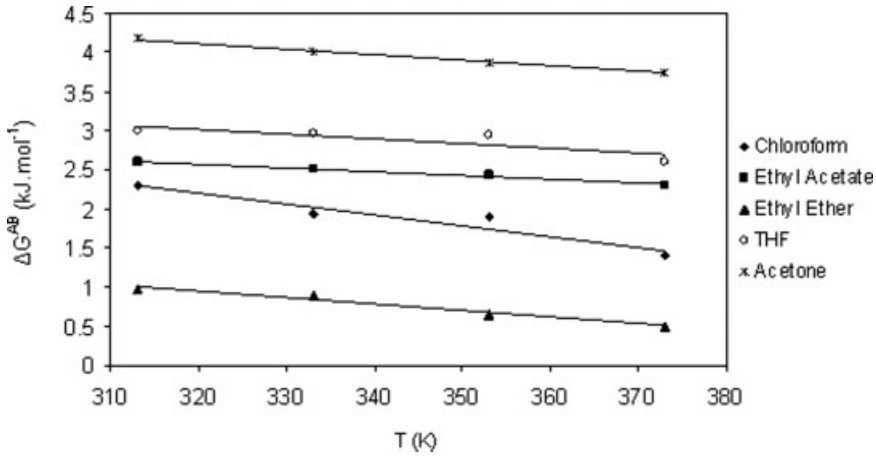

FIG. 11. Plot of free energy of adsorption ΔG^{AB} versus temperature for untreated hemp fiber.

ilar to those obtained for organic materials in other works [15, 27]. The results show that the SMA Imide-treated fibers had slightly higher dispersive force compared with nontreated fibers. This is because treatment of fibers with SMA Imide increases the dispersive component of the surface because of the presence of the nonpolar phenolic groups in the SMA component.

Acid–Base Interaction. To get an estimation of the acid–base surface properties of the fibers, the free energy of adsorptions at a given value of $a\left(\gamma_1^d\right)^{1/2}$, which is the difference between the point corresponding to the specific probe and the reference line, must be determined. Thus, the vertical distances of the acidic, basic, and amphoteric probes from the alkane line correspond to Gibbs free energy of adsorption due to acid–base interactions. This distance is calculated for each probe and plotted versus temperature (Fig. 11).

The enthalpy of adsorption (ΔH^{AB}) corresponding to the acid–base interactions was determined by the intercept of the variation of ΔG^{AB} versus temperature, according to *Eq*. 8. When ΔH^{AB} is known, the acid–base characteristic of the fibers can be obtained using *Eq*. 9 and plotting ΔH^{AB}/AN versus DN/AN. The variations were almost linear for both untreated and SMA Imide-treated fibers, as shown in Fig. 12. The K_A and K_B values for the fibers were estimated from the slope and intercept of the linear regression lines of ΔH^{AB}/AN versus DN/AN. These values are shown in Table 3.

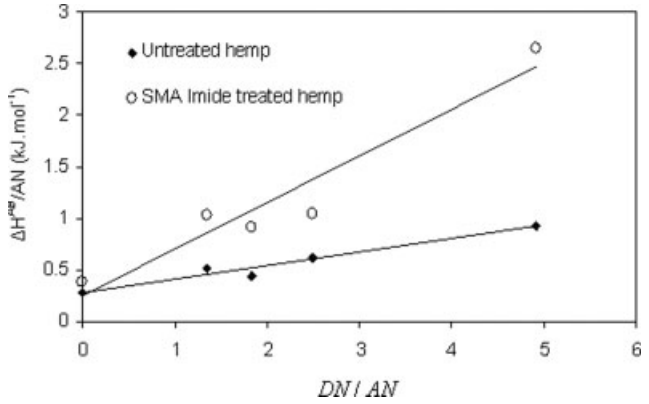

FIG. 12. Plot of ΔH^{AB}/AN vs. DN/AN.

The untreated hemp fiber showed an amphoteric surface characteristic with a predominantly basic characteristic, which can be because of the presence of extractives, such as triglycerides, that expect to show a pronounced basic behavior [27]. Modification of fibers with SMA imide resin slightly decreases the basic character of hemp fibers, which could be due to the dissolution of extractives during the treatment. The acid character of hemp fiber also increased significantly, possibly because of exposure of more cellulose, which is predominantly acidic, and presence of amino groups from the SMA component that has acidic behavior. This result indicates that the acid–base interactions with the acrylic resin increased for SMA-treated fibers. As it was found before, composites manufactured with SMA-treated fibers showed significant improvement in mechanical properties compared with untreated fibers. This could be explained because of the improvement of the acid–base interaction, which results in enhancing the interfacial adhesion of the hemp fiber and matrix.

Pull-Out Test

The pull-out test was used for measuring the interfacial bond strength between the hemp fibers and acrylic resin,

TABLE 3. Acid–base character of the hemp fibers.

Type of fiber	K_A	K_B
Untreated hemp	0.13	0.27
SMA imide treated hemp	0.45	0.24

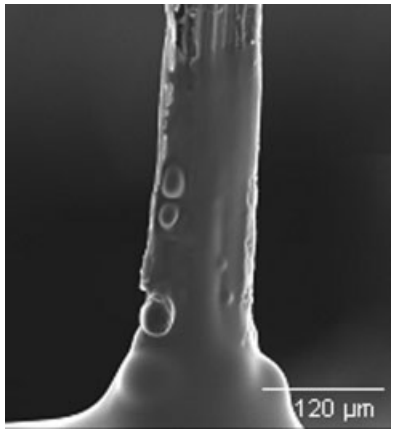

FIG. 13. SEM image of the pull-out specimen.

and thus yielding an estimation of the adhesion. This test measures the force, F_{max}, required to pull out a fiber whose end is embedded in a matrix. The F_{max} is then converted into the apparent mean interfacial shear strength, τ_i according to the following equation [11]:

$$\tau_i = \frac{F_{max}}{\pi D L_e} \tag{10}$$

where F_{max} is the maximum tensile load, D is the fiber diameter, and L_e is the embedded fiber length.

In general, for strong interfacial strength, an increasingly higher percentage of fibers are broken without being pulled out, and a larger experimental scatter is observed. Furthermore, when imbedded fibers are too long, the fiber is broken prior to pulling-out, which means no data can be recorded. In this research, most of the samples with a longer embedded length (>0.8 mm) of fibers did not show any pull-out phenomenon, and the fibers were fractured at a maximum force. However, as the embedded length was reduced below 0.7 mm, most of the fibers were pulled out. The pull-out was confirmed by visual inspection of the test samples. Figure 13 shows a SEM image of the specimen before the pull-out test. The meniscus at the fiber entry point into resin is clear. This is probably because of resin penetration into the micropores at the surface of fiber and the capillary rise effect.

The fiber behavior in the pull-out experiment can be divided in two main groups, fiber pull-out and fiber breakage. Close investigation of the data obtained from the pull-out test results shows that applied loads for the broken fibers are much higher than that for the pulled-out fibers regardless of the treated and untreated fibers. Calculated normal stresses of the broken fibers are also less than the yield or fracture strength of single hemp fibers. Therefore, in most of them failure occurred before fibers reach its yield strength, which is probably because of inhomogeneous nature of the hemp fiber and the presence of some defects on the surface of fiber. It can also be because of the occurrence of defects during the preparation of pull-out specimens and the misalignment of fibers during the pull-out test.

There are three modes of failure when a fiber is pulled out from a matrix: adhesive failure at the interface, cohesive failure of the matrix close to the interface, and cohesive failure of the fiber close to the interface [16]. After pull-out tests, specimens were analyzed by SEM to evaluate the failure mode. Figure 14 shows SEM images of a treated pull-out fiber (a) and higher magnified image of the debonded area (b). Before any debonding, the stress on the fiber at entry point of the meniscus to the polymer is maximum [20]. Therefore, it is probable that a crack is originated in the matrix in the meniscus region, where stress concentrations are the highest. The crack then likely reaches the interface and extends along the fiber.

In the pulled-out fibers, there are a number of sources of errors in calculating the interfacial bonding strength (shear strength). First, before fiber/matrix debonding, a crack propagates through the matrix that results in fracture of the matrix. Therefore, a part of the applied force is used for matrix failure; however, the amount of the force is negligible (~1 g). Second, there is a possibility of the fiber fracture inside the embedded portion of the fiber for both treated and untreated fibers. In this case, a part of the applied force consume for the fracture of fiber. Moreover, because of difficulties of measuring the exact embedded surface area for each fiber, it is assumed that the fibers are perfectly in a cylindrical shape with smooth surface, which may not be completely valid and it affects the accuracy of calculation. Thus, interfacial shear stresses calculated from pull-out tests can be used only to estimate the bonding strength and compare the effect of the treatment on the fiber/matrix interfacial bonding strength.

Figure 15 illustrates an example of the load-extension curve for hemp fiber/acrylic system in pull-out test. The curve shows that the measured force increases until a maximum and drops after the debonding is completed. After debonding, the load suddenly decreases and there is a small constant frictional force.

Figure 16 shows the calculated mean interfacial bonding strength for the untreated and SMA-treated samples obtained from the pull-out test. The ANOVA statistical

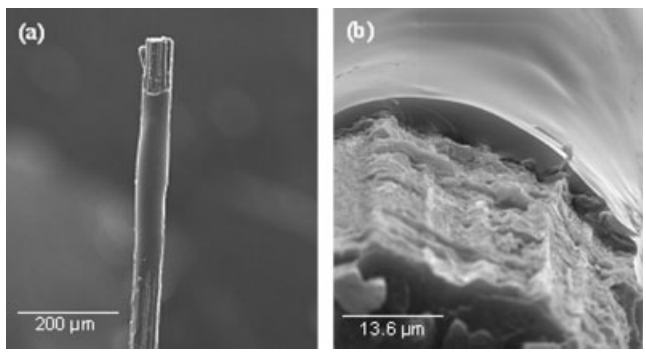

FIG. 14. SEM images of the specimen after the pull-out test.

 DOI 10.1002/pc

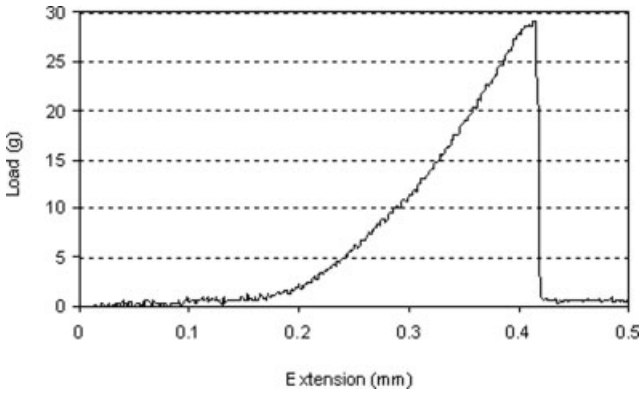

FIG. 15. Load-extension curve for hemp/acrylic pull-out specimen.

analysis shows the difference of τ_i value calculated for treated and untreated fibers is statistically significant at a 95% confidence level. The estimated average stress to pull the SMA treated fibers out was 71% higher than that calculated for untreated fibers. The higher interfacial strength for the treated fibers shows that the SMA treatment had a beneficial influence on the adhesion of the acrylic resin into hemp fibers. This may be explained because the dispersive component and the acid character of the fibers treated with SMA Imide resin increased, as discussed previously. This leads to an increased interfacial adhesion between hemp fiber and acrylic polymer. Because of improved interfacial interactions, the resin is expected to spread better on the surface of fibers. This will reduce the number of voids and bubbles at the interface, which are commonly present in all types of composites. When a composite is loaded, these voids act as stress concentration points, often leading to failure of the specimen. Therefore, better spreading and wetting is expected to improve the interfacial adhesion.

SUMMARY

Treatment of hemp fibers with SMA Imide resin enhanced the fiber/matrix adhesion and consequently the performance of the composite significantly, compared with the untreated composite. The dispersive component of surface energy for untreated hemp fibers was found to be 37 $mJ \cdot m^{-2}$ at 313 K using IGC. The results show that the SMA Imide resin treated fibers has slightly higher dispersive force compared with untreated fibers because of the presence of nonpolar phenolic groups. The untreated hemp fiber shows an amphoteric surface characteristic with a predominantly basic characteristic, which can be due to the presence of extractives such as triglycerides. Modification of fibers with SMA Imide resin was found to slightly decrease the basic character of hemp fibers, which can be due to dissolution of extractives during the treatment. On the other hand, the acid character of hemp fiber increased significantly. This change can be because of the exposure of more cellulose, which is predominantly acidic and also presence of amino groups from the SMA component that has acidic behavior. From these results, it can be expected that the acid–base interactions with the acrylic resin increased for SMA treated fibers that results in enhancing the interfacial adhesion of the hemp fiber and matrix. The effect of SMA Imide treatment on the tensile properties of the fiber was investigated. It was observed that there is no significant difference between the strength of untreated and treated fibers. To estimate the adhesion, the pull-out test was performed to measure the interfacial bond strength between the hemp fibers and acrylic resin. The average estimated interfacial strength for the SMA treated fibers is 71% higher than the one obtained for untreated fibers. The higher interfacial strength for the treated fibers shows that the SMA treatment had a beneficial effect in the adhesion of the acrylic resin into hemp fibers.

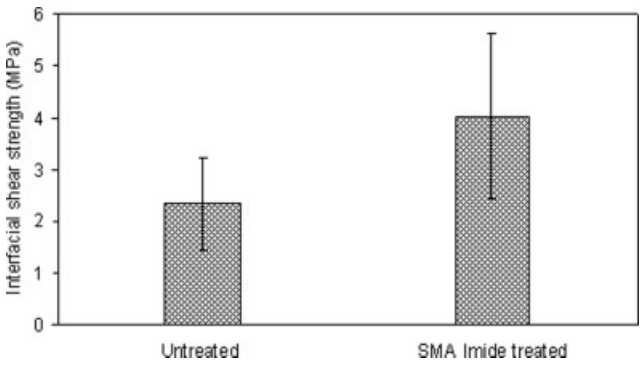

FIG. 16. Interfacial shear strength obtained for untreated and SMA Imide treated fibers.

REFERENCES

1. P. Mapleston, *Mod. Plast.*, **76**, 4 (1999).
2. S.V. Joshi, L.T. Drzal, and A.K. Mohanty, *Compos. A*, **35**, 3 (2004).
3. A.K. Mohanty, M. Misra, and L.T. Drzal, *J. Polym. Environ.*, **10**, 1 (2002).
4. L.Y. Mwaikambo and M.P. Ansell, *J. Appl. Polym. Sci.*, **84**, 12 (2002).
5. G. Cantero, A. Arbelaiz, and R. Llano-Ponte, *Compos. Sci. Technol.*, **63**, 9 (2003).
6. P. Gañán, J. Cruz, and S. Garbizu, *J. Appl. Polym. Sci.*, **94**, 4 (2004).
7. G. Mehta, L.T. Drzal, and A.K. Mohanty, *J. Appl. Polym. Sci.*, **99**, 3 (2006).
8. A. Voelkel, *Chemom. Intell. Lab. Syst*, **72**, 2 (2004).
9. U. Panzer, *Colloids Surf.*, **57**, 2 (1991).
10. D.P. Kamdem, *Langmuir*, **9**, 3039 (1993).
11. M.A. Tshabalala, *J. Appl. Polym. Sci.*, **65**, 5 (1997).
12. D. Gulati, "Modification of Interface in Natural Fiber Reinforced Polymer Composites", Master Thesis, University of Toronto (2005).
13. L. Ferreira, M.B. Evangelista, M. Martins, and L. Cristina, *Polymer*, **46**, 23 (2005).

14. M. Kazayawoko, J.J. Balatinecz, and L.M. Matuana, *J. Mater. Sci*., **34**, 24 (1999).
15. N. Chand and P.K. Rohatgi, *Polym. Commun*., **27**, 157 (1986).
16. T.H.D. Sydenstricker, S. Mochnaz, and S.C. Amico, *Polym. Test*., **22**, 4 (2003).
17. T. Behzad, M. Sain, U. S. Patent 0,245,161 (2005).
18. Annual books of ASTM standards, American Society for Testing and Materials, Philadelphia, Pa, **08**, 01 (2005) 50.
19. Annual books of ASTM standards, American Society for Testing and Materials, Philadelphia, Pa, **08**, 01 (2005) 149.
20. M.R. Piggott, *Load Bearing Fibre Composites*, Kluwer, Boston (2002).
21. F.M. Fowkes and M. Mostafa, *Ind. Eng. Chem. Prod. Res. Dev*., **17**, 1 (1978).
22. H.M. McNair, "Instrument Overview (Ch. 2, p. 14) and Basic Concepts and Terms (Ch. 3, p. 29)," in *Basic Gas Chromatography*, J.M. Miller, Ed., Wiley, New York (1998).
23. L.R. Lloyd, "Determination of Fiber-Matrix Adhesion and Acid-Base Interactions," in *Inverse Gas Chromatography: Characterization of Polymers and Other Materials*, American Chemical Society, Washington, DC, 217 (1989).
24. J. Schultz, L. Lavielle, and C. Martin, *J. Adhes*., **23**, 45 (1987).
25. M. Kazayawoko, J.J. Balatinecz, and M. Romansky, *J. Colloid Interface Sci*., **190**, 2 (1997).
26. F.M. Fowkes, *Ind. Eng. Chem*., **56**, 12 (1964).
27. D. Gulati and M. Sain, *Polym. Eng. Sci*., **46**, 3 (2006).

 DOI 10.1002/pc